Characterization of alkaloids and metabolic intermediates from *Dendrobium officinale* induced by methyl jasmonate

Cheng Song[1#], Yunpeng Zhang[2#], Muhammad Aamir Manzoor[3], Qing Jin[3*], Guohui Li[1*]

[1] *College of Biological and Pharmaceutical Engineering, West Anhui University, Luan, China*

[2] *Shanghai Key Laboratory of regulatory biology, School of Life Science, East China Normal University, Shanghai, China*

[3] *College of Life Science, Anhui Agricultural University, Hefei, China*

[#] *Contributed equally to this article*

***Correspondence:**

Dr. Guohui Li

Affiliation: West Anhui University

Address: West Moon Island, Yunlu Bridge, Lu'an, Anhui, 237012, China

Email: 2352871552@qq.com

Prof. Qing Jin

Affiliation: Anhui Agricultural University

Address: No. 130 Changjiang West Road, Hefei, Anhui, 230036, China

Email: qingjin@ahau.edu.cn

Abstract

JA signaling plays a pivotal role in plant stress responses and secondary metabolism. Many studies have demonstrated that jasmonates effectively induce the expressions of alkaloid biosynthesis genes in various plants, which rendered to the accumulation of alkaloid to counteract stresses. Despite the multiple roles of JAs in the regulation of plant growth and different stresses, less studied involved in the regulatory role of JA in *Dendrobium officinale*. Here, a strategy for the rapid identification of alkaloid and precursors of *D. officinale* was established based on a solid-phase extraction-high performance liquid chromatography-linear ion trap- Orbitrap tandem mass spectrometry (SPE-HPLC-LTQ-Orbitrap) method. The potential compounds were tentatively identified by aligning the accurate molecular weight with the METLIN and Dictionary of Natural

Products databases. The chemical structures and main characteristic fragments of the potential compounds were further confirmed by retrieving the multistage mass spectra from the MassBank and METLIN databases.The Mass Frontier software was used to speculate the fragmentation pathway of the identified compounds. As a result, seven alkaloids were separated and identified from *D. officinale,* which were mainly classified into five types (tropane alkaloids, tetrahydroisoquinoline alkaloids, quinolizidine alkaloids, piperidine alkaloids and spermidine alkaloids). Besides the alkaloids, forty-nine chemical substances, including guanidines, nucleotides, dipeptides, sphingolipids and nitrogen-containing glucosides, were concurrently identified in the experiment. Taken together, this study revealed the composition of chemicals currently found in *D. officinale*, which could provide the scientific method for the identification of alkaloids in other Dendrobium plants.

Keywords: JA signaling, Liquid chromatography-mass spectrometry, Alkaloid, Fragmentation, *Dendrobium officinale*

Introduction

Traditional Chinese medicine (TCM) involves complex chemical constituents. An effective determination of one group of metabolites from a certain plant entails a comprehensive methodology for their purification and identification. Conventional detection methods such as thin-layer chromatography (TLC) and high-performance liquid chromatography (HPLC) generally provide such low accuracy and poor sensitivity that leading to incapable of detecting some trace substances (Pan et al., 2015). A separation and identification method with strong specificity, high efficiency, and few interference is urgently needed. Solid-phase extraction (SPE) was usually used for the complicated specimens by reducing matrix interference and raising sensitivity (Bucar et al. 2013). Orbitrap mass spectrometry is one kind of high- resolution mass analyzer containing high-resolution multistage mass fragment monitoring, a selective fragmentation mode, and a personalized data acquisition method (Qiu et al. 2015). Orbitrap has been widely applied in pharmacokinetic analysis, food industry, environmental monitoring and proteomics (Anastasia et al. 2013; Rada et al. 2015; Haddad and Kümmerer 2014; Li et al. 2013). Therefore, the SPE-HPLC-LTQ-Orbitrap technique is proved to be a powerful means to elucidate the complicacy in TCM. *Dendrobium officinale* Kimura et Migo, as a type of perennial herb, is attached to the

58 Dendrobium genus of Orchidaceae. As a valuable TCM, *D. officinale* contains many different
59 types of active ingredients, including polysaccharides, alkaloids, bibenzyls, phenanthrenes,
60 sesquiterpenoids, fluorenones, flavonoids, steroids, etc. (Xu et al. 2013). Some of these
61 compounds had exhibited versatile pharmacological and pharmacodynamic activity (Ng et al.
62 2012). The earliest study on the alkaloids of the Dendrobium genus started from dendrobine of *D.*
63 *nobile*. For the decades, dozens of alkaloids have been subsequently identified from *D. anosmum*
64 (Leander and Lüning 1968), *D. chrysanthum* (Ekevåg et al. 1973), *D. crepidatum* (Elander et al.
65 1973), *D. findlayanum* (Granelli et al. 1970), *D. friedricksianum* (Hedman et al. 1971), *D.*
66 *hilderbrandii* (Elander and Leander 1971), *D. loddigessi* (Li et al. 1991), *D. lohohense* (Inubushi
67 et al. 1964), *D. moniliforme* (Liu et al. 2007), *D. parishii* (Leander and Lüning 1968), *D. pierardii*
68 (Elander et al. 1971), *D. primulimun* (Blomqvist et al. 1972), *D. snowflake* (Morita et al. 2000)
69 and *D. wardianum* (Glomqvist et al. 1973). At present, the alkaloids identified from Dendrobiun
70 plants had been divided into five categories based on their chemical structures, including
71 sesquiterpenoid alkaloids, indolizidine alkaloids, pyrrolidine alkaloids, phthalide alkaloids, and
72 imidazole alkaloids (Xu et al. 2013).
73 Thus far, the composition and biosynthetic pathway of the alkaloids in *D. officinale* has not
74 been entirely understood. The determination of the alkaloids between *D. officinale* and *D. nobile*
75 using an LC-MS method showed that 25 identical compositions in the two Dendrobium plants
76 were tentatively identified; however, dendrobine was only detected in *D. nobile* (Chen et al. 2006).
77 Using a UPLC method, a few coumarins, alkaloids and bibenzyl components from fifteen
78 Dendrobium species were quantitatively determined. Dendrobine was only detected in *D. nobile*
79 originated from the Guizhou and Yunnan Provinces (Xu et al. 2010). The genome and
80 transcriptome analyses of *D. officinale* implied that a biosynthetic pathway oriented to the
81 terpenoid indole alkaloids likely exists (Guo et al. 2013; Yan et al. 2015). Recently,
82 high-throughput sequencing revealed the identification of a total of 56 genes, including 25 key
83 enzymes potentially involved in the synthesis of terpenoid indole alkaloids, tropine alkaloids and
84 isoquinolines alkaloids in *D. officinale* (Niu et al, 2021). Many studies have shown that *CrMYC2*
85 and *ORCAs* transcription factors play a positive role in elevating the TIAs content in *Catharanthus*
86 *roseus* (Memelink and Gantet 2007). With the help of transcriptome sequencing, 75 bHLH family
87 genes and 66 AP2/ERF genes were identified in the DEGs of *D. officinale,* suggesting that those

88 transcription factors could be involved in the regulation of secondary metabolism, especially in
89 TIAs biosynthesis (Zhang et al. 2016). Mevalonate (MVA) and methylerythritol 4-phosphate
90 (MEP) pathway are both core pathways related to MeJA-induced accumulation of TIAs. In *D.*
91 *officinale*, the key genes in MVA and MEP pathway and some post-modified enzymes were
92 significantly up-regulated by MeJA treatment (Chen et al. 2019). In the previous study,
93 high-yielding production of alkaloids from *D. officinale* were obtained with the combination of
94 tryptophan, secologanin and MeJA treatment (Jiao et al. 2018). Here, a technical scheme for the
95 separation and determination of alkaloids and precursors in *D. officinale* was established. The
96 accurate mass weights of the components separated by HPLC were determined using an Orbitrap
97 mass analyzer. The multistage fragmentation mass spectra of alkaloids were monitored to
98 speculate the potential substances based on a database-dependent retrieval method. Alkaloid and
99 their precursors related to alkaloid-synthetic pathway were associated to construct the metabolic
100 network between upstream and downstream. The results would provide a reliable scientific
101 reference and technical guidance for the development and quality evaluation of *D. officinale*.

102 Materials and Methods

103 Instruments and chemicals

104 The LTQ-Orbitrap XL mass spectrometer were manufactured by Thermo Fisher Scientific
105 (Bremen, Germany). The Agilent 1260 instrument used in the experiments was manufactured by
106 Agilent Technologies (Waldbronn, Germany). The Xcalibur (*v.* 2.1) and Mass Frontier (*v.* 6.0)
107 were used for the analysis of mass spectrometry and speculation of the fragmentation pathways .
108 Acetonitrile and formic acid were of HPLC grade. Other chemicals were domestically made
109 analytical reagents. The standards of reserpine and sarpagine was obtained from Aladdin
110 (Shanghai, China) and BioBioPha (Kunming, China), respectively.

111 Plant materials preparation

112 The *D. officinale* samples used in the experiment were obtained from the tissue culture room
113 of the Plant Cell Engineering Center in West Anhui University. The tissue-cultural seedlings
114 cultivated in MS medium were collected after 100 μM MeJA treatment. The seedlings were firstly
115 dried at 110 °C for 15 min and kept in a constant weight at 60 °C. The dried materials were ground
116 into powders by a universal grinder. Using the ultrasonic extraction method, two gram of powder

117 was placed in a round-bottom flask with 100 mL of methanol and extracted three times at room
118 temperature. The bromocresol green colorimetric method was used for the determination of total
119 alkaloids (Chen et al. 2019). The extraction solution was centrifuged for 10 min at 6000 x *g* to get
120 the supernatant, then evaporated to dryness in a rotary evaporator. The extraction was dissolved
121 with 5 mL of dilute sulfuric acid, filtered through a 0.22 μm membrane, and pretreated using
122 MCX cartridges (60 mg, 3 mL) for purification. The protocol was successively conducted by our
123 previous method (Song et al. 2020).

124 # Experimental conditions

125 The Waters T3 column (150 mm × 4.6 mm, 3 μm) was used for the chromatographic
126 separation. The mobile phases acetonitrile (A) with 0.1% formic acid and aqueous phase (B) with
127 0.1% formic acid were used for the experiment. Gradient elution process was as follows: 0-2 min
128 (0% A), 2-12 min (0 to 15% A), 12-22 min (15 to 35% A), 22-32 min (35 to 80% A), and 32-37
129 min (80 to 0% A). The UV wavelength was set at 280 nm, and the column temperature was set at
130 25 °C. A three-way splitter was connected with the mass analyzer at a 0.3 mL min^{-1} flow rate. The
131 ion-source parameters were refereed to Kumar's method and slightly modified (Kumar et al.,
132 2015). The detailed parameters were as follows: sheath gas at 25 arb, auxiliary gas at 3 arb, spray
133 voltage at 4 kV, the capillary temperature at 320 °C, tube lens at 120 V, and capillary voltage at 30
134 V. The MS data were collected at $100 \leq m/z \leq 1000$ in positive-ion mode. Two data acquisition
135 methods were used in the experiments. In one method, a high-resolution scan was conducted using
136 the Orbitrap mass analyzer to acquire the MS data at a resolution at 30,000 FWHM and the MS^2
137 data at 15,000 FWHM. A data-dependent MS^n scan was used for the analysis of the MS^2 spectra
138 generated from the most abundant ions of the MS spectra. In the other method, a high-resolution
139 scan was conducted first to acquire the MS data at a resolution at 30,000 FWHM, then the LTQ
140 dynode was used to scan the MS^2 and MS^3 spectra. The dynamic exclusion function was used to
141 reduce repeat scans, and the repeat count was 2. The exclusion duration was 20 s, and the
142 exclusion mass width was 3 *m/z*. The suitable collision-induced dissociation (CID) energy was set
143 at 35%. The minimum signal threshold was 500, and the isolation width of precursor ions was 2
144 *m/z.* Sarpagine and reserpine were respectively injected into the mass analyzer via a syringe pump
145 at a flow rate of 6 μL min^{-1} to complete the direct infusion analysis. The putative molecular

formulae were calculated and obtained according to the accurate molecular weight using Xcalibur (*v.* 2.1). Compounds were tentatively identified by matching METLIN, Mass Bank, Dictionary of Natural Products and Chemspider databases. For the compounds without multiple mass spectra, Mass Frontier (*v.* 6.0) was helped to speculate and deduce the fragmentation pathway.

Results and discussion

Biomass and alkaloid contents under the MeJA treatment

The effects of methyl jasmonate on the growth and alkaloid accumulation of *D. officinale* was studied. The results showed that MeJA delayed the growth rate of *D. officinale* and initiated the synthesis of a large number of alkaloids in logarithmic growth phase (**Fig.1**). The highest content of alkaloids climaxed to 343 μg/g when cultured on the 32 days. After that, the fresh weight tended to be stable, and the alkaloid content began to fall gradually. The results suggested that jasmonates could continuously promote the synthesis of alkaloids during the growth of *D. officinale*. The growth trend and accumulating pattern were consistent with our previous study (Jiao et al. 2018).

Mass spectra interpretation

Firstly, *D. officinale* samples were extracted by methanol and dissolved with diluted sulfuric acid. The MCX cartridges were used for the purification of alkaloids from the acidic aqueous extraction. To optimize the condition of mass spectrometry, the suitable CID energy was achieved by the direct infusion experiment. Generally, the strongest fragment ions and the smallest number of fragments were observed at 30-35% collision energy, whereas the abundances of the fragments decreased substantially at 45% or greater collision energy (Song et al. 2020). In this experiment, sarpagine and reserpine achieved sufficient fragments both in quantity and intensity at 40% collision energy. High-resolution mass analysis was conducted by a data-dependent MS^n scan from the workstation to produce abundant fragmentation spectra of the product ions. Due to the high resolution, the scan rate of a single spectrum was reduced, and the analytical analysis time of the entire sample was extended. An appropriate exclusion duration time was required for the dynamic exclusion function to avoid repeat scans of target ions and thereby shorten the analysis time of the samples (Zhang et al. 2012). Another important function of dynamic exclusion was to obtain the fragment information of the co-eluting small peaks, which allowed compounds with

175 low ionized potentials to be detected (Pan et al. 2015). The total ion current chromatogram of the
176 methanol extract spiked with standards from *D. officinale* is presented, as obtained in the
177 positive-ion mode under the optimized mass parameters and analytical conditions (**Fig.S1a**).
178 Generally, $[M+H]^+$ or $[M]^+$ was achieved through the soft ionization in the positive mode. The
179 molecular-ion peaks of sarpagine and reserpine were separately extracted at *m/z* 311.1738 and
180 609.2772. The retention time of sarpagine and reserpine were at 12.95 min and 25.41 min,
181 respectively (**Fig. S1b** and **S1c**). The results indicated that the established method for the mass
182 spectrometry was suitable for the separation and characterization of alkaloids.
183 Using a data-dependent MS^n scan method, the MS spectra of two standards were obtained
184 from the Orbitrap analyzer, and the MS^n spectra were obtained from the LTQ. It was indicated that
185 the π bonds on the indole groups of sarpagine and reserpine were easily dissociated to produce
186 $[M+H]^+$ peaks and produced massive hydrogen rearrangement. The ionization and electron
187 transfer were observed on the position of the group cleavage because of the induced dissociation
188 effect of the high-energy collisions. The putative fragmentation modes of sarpagine and reserpine
189 are presented in Fig. S2 and S3. The characteristic fragments with *m/z* 146 and 174 from the
190 indole group were produced by the cleavage of sarpagine and reserpine, respectively. The
191 characteristic ion *m/z* 195 cleaved on the ester bond was obtained to produce the
192 3,4,5-trimethoxybenzaldehyde group from the aglycone. Finally, forty-nine nitrogen-containing
193 compounds, including seven alkaloids, were separated and tentatively identified from *D. officinale*
194 (**Table S1**).

195 Identification of the alkaloids

196 The small molecular compounds previously identified from *D. officinale* mainly include
197 stilbenoids (bibenzyl and phenanthrene), phenols, lignans, nucleotides, lactones, flavonoids,
198 steroids, and fatty acids (Chen et al. 2013). Based on the high resolution and sensitivity of
199 LTQ-Orbitrap for the trace substances, coupled with the high selectivity of MCX for the
200 medium-strength alkaline compounds, seven alkaloids identified from the methanol extract of *D.*
201 *officinale* were divided into five classes based on the chemical structure, including tropane
202 alkaloids, tetrahydroisoquinoline alkaloids, quinolizidine alkaloids, piperidine alkaloids, and
203 spermidine alkaloids. The special fragmentation modes of different alkaloids in the ESI source

204 were discussed below.

205 The tropane alkaloids consist of pyridine conjugated with piperidine. The experiment
206 involved in DART-MS in-source CID at 90 V indicated that the characteristic ions of tropine were
207 *m/z* 158, 142, 124, 93, and 67 (Lesiak et al, 2015). 2,3-Dihydroxynortropane was a kind of
208 nortropane-type alkaloid that lacks an N-methyl group (Asano et al, 2001). Notably, the hydroxyl
209 groups were present on its C-2 and C-3 in both the α- and β-configurations, as confirmed by a
210 benzoate chirality method (Kusano et al. 2002). In this study, a strong $[M+H-\cdot OH]^+$ ion peak was
211 observed under the set CID conditions. In addition to the characteristic ions *m/z* 93 and 67,and the
212 stronger fragments *m/z* 113, 98 and 82 were observed (**Fig. 2a**). The MS^2 and MS^3 spectra of
213 2,3-dihydroxynortropane were displayed, and $[M+H-\cdot OH]^+$ ion also appeared (**Fig. 2b** and **2c**).
214 However, the base peak of 2,3-dihydroxy- nortropane was the 2-methylpyrrole ion, which was
215 further fragmented to get *m/z* 56. Finally, the compound was identified as
216 2,3-dihydroxynortropane or its isomers.Two tetrahydroisoquinoline alkaloids were identified as
217 alamaridine and 1,2-dihydro-*O*-methyltazettine. The characteristic ions of tetrahydroisoquinoline
218 group in alamaridine were *m/z* 177, 176, and 162 in the EI source, and the methyl group on C-5
219 was easier to lost compared to that on C-10 (Bhattacharjya et al. 1988). The MS^2 and MS^3 spectra
220 of alamaridine are displayed respectively (**Fig. 3a** and **3b**). These spectra indicated that the methyl
221 groups on C-5 and C-10 were lost to produce the base peaks $[M+H-2CH_3-3H]^+$, which further
222 lacked a hydroxyl group to generate *m/z* 248 in the MS^3 spectrum. The C_2H_3 and ·OH groups were
223 successively cleaved to generate *m/z* 221 and 204 on ring B and *m/z* 176 and 161 on ring C.
224 1,2-Dihydro-*O*-methyltazettine, also known as ungvedine, is a tazettine- type alkaloid (Kadyrov et
225 al. 1979). The main fragments *m/z* 207 and 142 were generated by 1,2-dihydro-*O*- methyltazettine
226 with equivalent intensity (**Fig. 3c**). The *m/z* 142 further lacked the methyl group and
227 simultaneously formed two double bonds to generate the base peak *m/z* 124 (**Fig. 3d**). Previous
228 studies have shown that the fragmentation pattern of tazettine-type alkaloid and its C_3H_7N group
229 was easily lost to produce the characteristic ion $[M+H-57]^+$ (Zhang et al. 2009). In Fig. 3c,
230 1,2-dihydro-*O*- methyltazettine was fragmented by RDA cleavage at both C-6, N-5 and C-4b,
231 C-6a. 1,2-Dihydro- *O*-methyltazettine was cleaved at C-4b, C-12a but not on C-3, C-4, and thus
232 did not produce $[M+H-C_3H_7N]^+$. There was a coordination bond between nitrogen and oxygen
233 presented in the quinolizidine alkaloid methyllagerine *N*-oxide. It was indicated that this bond

234 easily led to the generation of the fragment $[M-O]^+$ in the EI source (Lee et al. 2011). The oxygen
235 was easily lost as well to produce the fragment *m/z* 437 in the ESI source (**Fig. 4a**). The
236 characteristic ions *m/z* 308 and 292 were generated by the cleavage of C-11 and C-22. According
237 to the different cleavage positions on ring B, the characteristic ions *m/z* 220 and 163 were also
238 generated. Meefarnine B was a spermidine alkaloid containing a polyamine heterocyclic ring.
239 These alkaloids are generally considered to be synthesized by putrescine, which is produced by
240 the degradation of L-arginine or L-ornithine (Silva et al. 2015). The MS^2 and MS^3 spectra of
241 meefarnine B indicate that the NH_3 group on N-5 was cleaved to produce the fragment *m/z* 421
242 under the collision dissociation effect (**Fig. 4b** and **4c**). The fragment *m/z* 292 was generated by
243 the cleavage of the side chain on N-9 and was further cleaved to produce *m/z* 218. Besides, the
244 fragment *m/z* 275 was generated by the cleavage of the *m/z* 421 on N-1 and C-2. The fragment *m/z*
245 204 was generated by the cleavage of the *m/z* 275 on N-9 and C-10, which further produced the
246 characteristic ion *m/z* 147. In this study, a piperidine alkaloid anapheline was tentatively identified
247 from *D. officinale*. The retention time of anapheline was 27.88 min, and the molecular weight of
248 the $[M+H]^+$ was 225.1945, which implies that its molecular formula was $C_{13}H_{25}ON_2$ (**Fig. S4**).
249 Anapheline easily lost H_2O to produce the fragment *m/z* 207 and the characteristic ion piperidine
250 *m/z* 100 during the collision-induced dissociation. The NH_3 group was lost to produce the *m/z* 83
251 in the MS^2 spectrum. Based on the MS^2 and MS^3 spectra, a presumed fragmentation pathway of
252 anapheline was proposed (**Fig. 5**).

253 # Identification of the guanidines

254 Three guanidine compounds were separated and determined from the methanol extract of *D.*
255 *officinale* for the first time. The MS^2 and MS^3 spectra of 4-guanidinobutanoic acid were displayed
256 respectively (**Fig. 6a** and **6b**). The mass spectra indicated that 4-guanidinobutanoic acid easily lost
257 H_2O to form the base peak *m/z* 128 and produced the characteristic ions *m/z* 104, 87 and 60. The
258 *m/z* 128 was further cleaved to produce the *m/z* 111 and 86. These results were consistent with
259 those reported by Nikolić et al. (Nikolić et al. 2012). Cyclocimipronidine is a cyclic guanidine
260 compound separated from *Cimicifuga racemosa*. Some studies showed that the characteristic ions
261 of cyclocimipronidine, a guanidine alkaloid in black cohosh, were the *m/z* 112, 95, 94, 70 and 67
262 (Gödecke et al. 2009) . In addition to the aforementioned characteristic ions, cyclocimipronidine

263 easily lost H_2O to generate the fragments *m/z* 136 and 84 (**Fig. 6c** and **6d**). The MS^2 and MS^3
264 spectra of *N-tert*-butyloxycarbonyl guanidine were displayed in Fig. 6e and 6f, respectively. It was
265 indicated that the characteristic ions were the *m/z* 142, 125, 104 and 87.

266 Identification of the nucleotides and derivatives

267 Nucleotides were composed of purine or pyrimidine linked with ribose. Adenosine, uridine
268 and guanosine had been separated from *D. officinale* in a previous study. In this study, five
269 nucleotide derivatives were tentatively identified. 2-Hydroxyadenine was an adenine derivative
270 that easily lost an NH_3 group to produce the characteristic ions *m/z* 135 and 110 (**Fig. S5a**). The
271 fragments *m/z* 107, 92 and 77 were generated in the MS^3 spectrum (**Fig. S5b**). Besides
272 2-hydroxyadenine, another four nucleotide derivatives were identified in the study. Their MS^2 and
273 MS^3 spectra indicated that the neutral loss of *m/z* 136 resulted from the loss of aglycones (**Fig. S5**
274 **c-j**). Comparison with the multistage mass spectra of the METLIN database
275 (https://metlin.scripps.edu/) resulted in the identification of adenosine, guanosine,
276 1-methyladenosine and cytidine.

277 Identification of the sphingolipids

278 Sphingolipid is a structurally complex lipid containing a long-chain sphingosine skeleton,
279 which forms the plasma and vacuole membranes of plant cells. Four phytosphingosines were
280 separated and identified from *D. officinale*. Because sphingosine contained some hydroxyl groups,
281 the characteristic ion $[M+H-H_2O]^+$ was observed during the dissociation (Fig. S6a-h). By aligning
282 against the Dictionary of Natural Products Database (http://dnp.chemnetbase.com), four
283 sphingolipids, including 2-amino-1,3-hexadecanediol, 2-amino-3-tetradecanol, 2-amino-1,3,4-
284 octadecanetriol and 2-amino-1,3,4-hexadecanetriol, were identified in the experiment.

285 Identification of the amino acids and their derivatives

286 Eight amino acids—L-lysine, L-histidine, L-arginine, L-valine, L-isoleucine, L-tyrosine,
287 L-phenylalanine and L-tryptophan—were identified from *D. officinale* based on accurate
288 molecular weights and the multistage mass spectra of standards from the MassBank
289 mass spectrum library (http://www.massbank.jp/QuickSearch. html) (**Table S1**). 4-Hydroxy-L-
290 threonine and urocanic acid were derivatives of L-threonine and L-histidine that easily lost H_2O to
291 produce the base peaks *m/z* 118 and 121. The putative fragment ions generated during their

292 cleavage were displayed in **Fig. S7a** and **S7b**, respectively. In addition to the derivatives of
293 L-threonine and L-histidine, four additional arginine derivatives were identified in this study.
294 N^2-Fructopyranosylarginine was an arginine monoglycoside and the byproduct generated by a
295 Maillard reaction between reducing sugars (fructose or glucose) and arginine upon heating
296 (Suzuki et al. 2004). Because fructose contained several hydroxyl groups, H_2O was easily lost to
297 produce the characteristic ions *m/z* 319, 301 and 283. The fragments *m/z* 257 and 239 were
298 produced by the cleavage of the guanidino group on the glycoside. N^2-Fructopyranosylarginine
299 was also cleaved to generate the characteristic ion *m/z* 175 on the N-glucosidic band and further
300 produced the aglycone *m/z* 158 via the neutral loss of fructose (**Fig. S7c-d**). The NH_3 group of
301 *N*-methylarginine was lost to produce the base peak *m/z* 172, as a result of the dissociation.
302 According to the different cleavages on the R group, the characteristic ions *m/z* 158, 133, 116 and
303 74 were generated (**Fig. S7e**). The characteristic ions *m/z* 126, 115, 97 and 70 were also generated
304 in the MS^3 spectrum by the cleavage of the *m/z* 172 fragment (**Fig. S7f**). The ·OH group of
305 N^{α}-acetylarginine was lost to produce the characteristic ion *m/z* 200. The fragments *m/z* 175 and
306 157 were generated by the different cleavages on the R group. The characteristic ions *m/z* 139, 115
307 and 70 were produced by the cleavage of amino and carboxyl groups linked with the chiral
308 carbons. The ·OH group of the *m/z* 200 was lost to produce the *m/z* 183 in the MS^3 spectrum, and
309 the other fragments were similar to those in the MS^2 spectrum (**Fig. S7g-h**).
310 N^2-(3-Hydroxysuccinoyl)arginine was formed by the substitution of the 3-hydroxysuccinoyl group
311 on the N-terminal of arginine. The typical feature of its cleavage was the loss of
312 3-hydroxysuccinoyl group to produce the characteristic ion *m/z* 175 (**Fig. S7i**), which was further
313 cleaved to generate the fragments *m/z* 158, 139 and 60 (**Fig. S7j**).

314 # Identification of the isomers

315 The accurate molecular weights of the compounds were provided by high-resolution mass
316 spectrometry, which allowed us to deduce the speculative molecular formulas. However, the
317 identification of isomers was less effective. Two pairs of isomers were identified in this study
318 based on their different retention times and distinct multistage fragments. The formula of both
319 L-homophenylalanine and β-phenyl-γ-aminobutyric acid was $C_{10}H_{13}O_2N$, but their retention times
320 were at 6.79 and 12.47 min, respectively (**Table S1**). The MS^2 spectra of L-homophenylalanine

321 and β-phenyl-γ-aminobutyric acid are displayed in **Fig. S8a** and **S8c**, respectively. These mass
322 spectra indicated that the NH_3 groups were easily lost to form the characteristic ion *m/z* 163.
323 However, the fragment *m/z* 120 produced in the spectrum of β-phenyl-γ-aminobutyric acid was
324 not observed in that of L-homophenylalanine. The MS^3 spectra presented different fragments,
325 which indicated two different compounds (**Fig. S8b** and **S8d**). The formula of both carbetamide
326 and N^{δ}-benzoylornithine were $C_{12}H_{16}O_3N_2$, but their retention times were at 9.77 and 14.93 min,
327 respectively (**Table S1**). The MS^2 and MS^3 spectra of carbetamide were displayed in **Fig. S8e** and
328 **S8f**, respectively. The MS^2 and MS^3 spectra of N^{δ}-benzoylornithine were displayed in Fig. S8g and
329 S8h, respectively. These two isomers exhibited different fragmentation patterns. The characteristic
330 ions of carbetamide were the *m/z* 120, 103 and 93 ions, whereas the characteristic ions of
331 N^{δ}-benzoylornithine were the *m/z* 219, 205, 175, 158 and 148 ions. The isomerism of the
332 dipeptides resulted from the chirality of the α-carbon and the different positions of peptide bonds
333 between two peptides. In the study, eight dipeptides were tentatively identified. Most of these
334 dipeptides had more than one retention time, suggesting that the isomers existed.

335 Identification of the nitrogen-containing glycosides

336 By comparing our spectra with the Metlin and Dictionary of Natural Products databases, we
337 tentatively identified four nitrogen-containing glycosides from *D. officinale*. The neutral loss of
338 H_2O in 5'-*O*-β-D-glucosylpyridoxine was easy to produce the characteristic ion *m/z* 314. The
339 fragment *m/z* 171 was generated by the cleavage on the O-glucosidic bond and further produced
340 the aglycone *m/z* 152 by the neutral loss of glucose (**Fig. S9a**). The H_2O on the aglycone of
341 4-*O*-β-D-glucopyranoside-2,4-benzoxazolediol was easily lost to produce the base peak *m/z* 296.
342 The benzoxazole ion *m/z* 136 was generated by the cleavage on the O-glucosidic bond (**Fig. S9b**).
343 The *m/z* 296 was cleaved to generate the characteristic ions *m/z* 119 and 94 (**Fig. S9c**). The MS^2
344 and MS^3 spectra of *O*-(tri-*O*-acetyl-α-L- rhamnopyranoside)- (4-hydroxybenzyl) methylcarbamic
345 acid were displayed in **Fig. S9d** and **S9e**, respectively. These mass spectra indicated that the
346 characteristic ion *m/z* 322 was generated by the cleavage of the ester bond and the side chain. The
347 *m/z* 322 was cleaved to produce the fragments *m/z* 304 and 160 in the MS^3 spectrum. Passicapsin
348 was composed of one glucose and a nitrogen-containing aglycone that easily produced the
349 aglycone *m/z* 238 via the neutral loss of glucose. The characteristic ions *m/z* 286 and 148 were

350 cleaved at the O-glucosidic bond between the side chain and the dideoxy glucoside (**Fig. S9f**). The
351 fragments *m/z* 148 and 106 in the MS^3 spectrum were produced by the cleavage of the aglycone
352 *m/z* 238 on the O-glucosidic bond. The H_2O of the aglycone *m/z* 238 was lost to produce the
353 fragments *m/z* 220 and 212, and the dideoxy glucoside group was further cleaved to generate the
354 *m/z* 190 and 174 (**Fig. S9g**).

355 The metabolic network and putative route of *D. officinale* 356 alkaloids

357 Generally, the biosynthetic pathways of alkaloids are derived from the catabolism of amino
358 acids. The biogenesis between the amino acids and the alkaloids has a relationship between
359 upstream and downstream upstream and downstream. In the experiment， many amino acids and
360 their derivatives were identified. The metabolic profile of the alkaloids in *D. officinale* was
361 constructed based on the KEGG pathway database. This profile indicated that the precursors of the
362 alkaloids were mainly L-phenylalanine, L-arginine, L-tyrosine and L-lysine (**Fig. 7**).
363 L-Phenylalanine was catalyzed by phenylalanine ammonialyase to form L-homophenylalanine.
364 3,4-Dihydroxybenzaldehyde was degraded by phenylalanine combined with tyramine to generate
365 norbelladine, which further formed 1,2-dihydro-*O*-methyltazettine via multistep biochemical
366 reactions. L-Arginine, as a major amino acid in *D. officinale*, was catalyzed by an
367 ethylene-forming enzyme to form guanidine, which was the precursor of three guanidine alkaloids.
368 L-arginine was also catalyzed by arginine amidinase to form L-ornithine, which was further
369 catalyzed by ornithine decarboxylase to generate putrescine. On the one hand, putrescine was the
370 precursor used for the synthesis of meefarnine B. On the other hand, putrescine was also catalyzed
371 by several enzymatic reactions to form tropine and 2,3-dihydroxynortropane. L-Lysine was
372 catalyzed by lysine decarboxylase to generate cadaverine, which further formed anapheline via a
373 four-step reaction.

374 Conclusion

375 The alkaloids and precursors of *D. officinale* with MeJA treatment were primarily studied by
376 the SPE-HPLC–LTQ-Orbitrap technique. The extraction and purification of the target compounds
377 was optimized, and the suitable conditions of ESI-CID-MS^n for the mass spectrometric detection
378 were established. Based on the accurate mass weight with MS^n fragmentation information

provided by the LTQ-Orbitrap mass spectrometer, forty-nine compounds, including amino acids derivatives, dipeptides, nucleotides, guanidines, alkaloids, sphingolipids and several nitrogen-containing glycosides, were tentatively identified from *D. officinale*. Seven alkaloids were identified from *D. officinale*. The combination of alkaloids and their precursors were associated to construct a metabolic network for the interpretation of biosynthetic pathways. These findings will serve as a technical guidance for the analyses and drug discoveries of *Dendrobium* alkaloids.

Author's contribution

CS and QJ discuss the writing plan. CS and YPZ draft the manuscript. CS, MAM and GHL edit the manuscript. GHL, CS and QJ acquire the funding.

Funding

This work was supported by Anhui Natural Science Foundation (2108085MC80), High-level Talents Research Initiation Fund of West Anhui University (WGKQ202001011, WGKQ2021079), and Quality Engineering Project of Anhui Provincial Department of Education (2020jyxm2137).

Declarations

Conflicts of interest

No interest to declare.

Consent to participate

All of the authors in this paper are informed content to participate in this manuscript.

Availability of data and material

All of the data including raw data sheets can be found in supplementary materials.

References

Asano N, Yokoyama K, Sakurai M, et al (2001) Dihydroxynortropane alkaloids from calystegine-producing plants. Phytochemistry 57:721–726. https://doi.org/https://doi.org/10.1016/S0031-9422(01)00131-5

Bhattacharjya, A., Mukhopadhyay, R., Pakrashi SC (1986) Structure and synthesis of alamaridine, a novel benzopyridoquinolizine alkaloid from alangium lamarck II. Tetrahedron Lett 27:1215–1216. https://doi.org/10.1016/S0040-4039(00)84220-3

Blomqvist L, Leander K, Lüning B, et al (1972) Studies on orchidaceae alkaloids. XXIX. The absolute configuration of dendroprimine, an alkaloid from Dendrobium primulinum Lindl. Acta chemica Scandinavica 26:3203-3206. doi:10.3891/acta.chem.scand.26-3203

Bucar F, Wube A, Schmid M (2013) Natural product isolation-how to get from biological material to pure compounds. Nat Prod Rep 30:525–545. https://doi.org/10.1039/c3np20106f

Chen X, Xiao S, Guo S (2006) Comparison of chemical compositions between Dendrobium candidum and Dendrobium nobile. Acta Academiae Medicinae Sinicae 28:524-529

Chen X, Wang C, Yang J, et al (2013) Research Progress on Chemical Composition and Chemical Analysis of Dendrobium officinale. Journal of Chinese Pharmaceutical ences, 48:1634-1640

Chen Y, Wang Y, Lyu P, et al (2019) Comparative transcriptomic analysis reveal the regulation mechanism underlying MeJA-induced accumulation of alkaloids in Dendrobium officinale. J Plant Res 132:419–429. https://doi.org/10.1007/s10265-019-01099-6

Da Silva G, Martinho A, Soengas RG, et al (2015) A new spermidine macrocyclic alkaloid isolated from Gymnosporia arenicola leaf. Fitoterapia 106:7–11. https://doi.org/10.1016/j.fitote.2015.07.020

Ekevåg U, Elander M, Gawell L, et al (1973) Studies on orchidaceae alkaloids. Part 33. Two new alkaloids, N-cis- and N-trans-cinnamoyl-norcuskhygrine from Dendrobium chrysanthum Wall. Acta chemica Scandinavica 27:1982-1986. doi:10.3891/acta.chem.scand.27-1982

Elander M, Gawell L, Leander K (1971) Studies on orchidaceae alkaloids. XXII. Synthesis and absolute configuration of pierardine. Lactone-betaine isomerization of shihunine. Acta chemica Scandinavica 25:721-724. doi:10.3891/acta.chem.scand.25-0721

Elander M, Leander K (1971) Studies on orchidaceae alkaloids. XXI. 6-hydroxynobiline, a new alkaloid from Dendrobium hildebrandii Rolfe. Acta chemica Scandinavica 25:717-720. doi:10.3891/acta.chem.scand.25-0717

Elander M, Leander K, Rosenblom J, et al (1973) Studies on orchidaceae alkaloids. XXXII. Crepidine, crepidamine and dendrocrepine, three alkaloids from Dendrobium crepidatum Lindl. Acta chemica Scandinavica 27:1907-1913. doi:10.3891/acta.chem.scand.27-1907

434 Glomqvist L, Brandänge S, Gawell L, et al (1973) Studies on orchidaceae alkaloids. XXXVII.
435 Dendrowardine, a quaternary alkaloid from Dendrobium wardianum Wr. Acta chemica
436 Scandinavica 27:1439-1441. doi:10.3891/acta.chem.scand.27-1439

437 Granelli I, Leander K, Lüning B (1970) Studies on orchidaceae alkaloids. XVI. A new alkaloid,
438 2-hydroxydendrobine, from Dendrobium findlayanum par. et Rchb. f. Acta chemica
439 Scandinavica 24:1209-1212. doi:10.3891/acta.chem.scand.24-1209

440 Gödecke T, Lankin DC, Nikolic D, et al (2009) Guanidine alkaloids and Pictet-Spengler adducts
441 from black cohosh (Cimicifuga racemosa). J Nat Prod 72:433–437.
442 https://doi.org/10.1021/np8006952

443 Guo X, Li Y, Li C, et al (2013) Analysis of the Dendrobium officinale transcriptome reveals
444 putative alkaloid biosynthetic genes and genetic markers. Gene 527:131–138.
445 https://doi.org/10.1016/j.gene.2013.05.073

446 Hedman K, Leander K, Lüning B (1971) Studies on orchidaceae alkaloids. XXV. N-isopentenyl
447 derivatives of dendroxine and 6-hydroxydendroxine from Dendrobium friedricksianum
448 Lindl. and Dendrobium hildebrandii Rolfe. Acta chemica Scandinavica 25:1142-1144.
449 doi:10.3891/acta.chem.scand.25-1142

450 Inubushi Y, Tsuda Y, Konita T, et al (1964) Shihunine: a new phthalide-pyrrolidine alkaloid.
451 Chemical & pharmaceutical bulletin 12:749-750. doi:10.1248/cpb.12.749

452 Jiao C, Song C, Zheng S, et al (2018) Metabolic profiling of Dendrobium officinale in response to
453 precursors and methyl jasmonate. Int J Mol Sci 19:. https://doi.org/10.3390/ijms19030728

454 Kadyrov KA, Abdusamatov A, Yunusov SY (1979) Ungvedine — A new alkaloid fromUngernia
455 vvedenskyi. Chemistry of Natural Compounds 15:513-514. doi:10.1007/BF00565070

456 Kalli A, Smith GT, Sweredoski MJ, Hess S (2013) Evaluation and optimization of mass
457 spectrometric settings during data-dependent acquisition mode: focus on LTQ-Orbitrap
458 mass analyzers. J Proteome Res 12:3071–3086. https://doi.org/10.1021/pr3011588

459 Kumar S, Singh A, Bajpai V, Kumar B (2016) Identification, characterization and distribution of
460 monoterpene indole alkaloids in Rauwolfia species by Orbitrap Velos Pro mass spectrometer.
461 J Pharm Biomed Anal 118:183–194. https://doi.org/10.1016/j.jpba.2015.10.037

462 Kusano G, Orihara S, Tsukamoto D, et al (2002) Five new nortropane alkaloids and six new
463 amino acids from the fruit of Morus alba Linne growing in Turkey. Chem Pharm Bull
464 50:185–192. https://doi.org/10.1248/cpb.50.185

465 Leander K, Lüning B (1968) Studies on Orchidaceae alkaloids. 8. An imidazolium salt from
466 Dendrobium anosmum Lindl. and Dendrobium parishii Rchb. f. Tetrahedron letters
467 8:905-908. doi:10.1016/s0040-4039(01)98823-9

468 Lee I, Youn U, Kim H, et al (2011) Biphenyl and biphenyl ether quinolizidine N -oxide alkaloids
469 from lagerstroemia indica L. Planta Med 77:2037–2041.
470 https://doi.org/10.1055/s-0031-1280064

471 Lesiak AD, Cody RB, Dane AJ, Musah RA (2015) Plant Seed Species Identification from
472 Chemical Fingerprints: A High-Throughput Application of Direct Analysis in Real Time
473 Mass Spectrometry. Anal Chem 87:8748–8757.
474 https://doi.org/10.1021/acs.analchem.5b01611

475 Li M, Hirata Y, Xu G, et al (1991) Studies on the chemical constituents of Dendrobium loddigesii
476 rolfe. Acta pharmaceutica Sinica 26:307-310

477 Li X, Shen B, Jiang Z, et al (2013) Rapid screening of drugs of abuse in human urine by
478 high-performance liquid chromatography coupled with high resolution and high mass
479 accuracy hybrid linear ion trap-Orbitrap mass spectrometry. J Chromatogr A 1302:95–104.
480 https://doi.org/10.1016/j.chroma.2013.06.028

481 Liu W, Hua Y, Zhan Z (2007) Moniline, a New Alkaloid from Dendrobium moniliforme. J Chem
482 Res 6:317–318. https://doi.org/10.1002/chin.200748193

483 Memelink J, Gantet P (2007) Transcription factors involved in terpenoid indole alkaloid
484 biosynthesis in Catharanthus roseus. Phytochem Rev 6:353–362.
485 https://doi.org/10.1007/s11101-006-9051-z

486 Morita H, Fujiwara M, Yoshida N, Kobayashi J (2000) New Picrotoxinin-type and
487 Dendrobine-type Sesquiterpenoids from Dendrobium Snowflake 'Red Star.' Tetrahedron
488 56:5801–5805. https://doi.org/https://doi.org/10.1016/S0040-4020(00)00530-5

489 Ng TB, Liu J, Wong JH, et al (2012) Review of research on Dendrobium, a prized folk medicine.
490 Appl Microbiol Biotechnol 93:1795–1803. https://doi.org/10.1007/s00253-011-3829-7

491 Nikolić D, Gödecke T, Chen SN, et al (2012) Mass spectrometric dereplication of
492 nitrogen-containing constituents of black cohosh (Cimicifuga racemosa L.). Fitoterapia
493 83:441–460. https://doi.org/10.1016/j.fitote.2011.12.006

494 Niu Z, Zhu F, Fan Y, et al (2021) The chromosome-level reference genome assembly for
495 Dendrobium officinale and its utility of functional genomics research and molecular
496 breeding study. Acta Pharm Sin B. https://doi.org/10.1016/j.apsb.2021.01.019

497 Pan H, Yang W, Zhang Y, et al (2015) An integrated strategy for the systematic characterization
498 and discovery of new indole alkaloids from Uncaria rhynchophylla by
499 UHPLC/DAD/LTQ-Orbitrap-MS. Anal Bioanal Chem 407:6057–6070.
500 https://doi.org/10.1007/s00216-015-8777-0

501 Quifer-Rada P, Vallverdú-Queralt A, Martínez-Huélamo M, et al (2015) A comprehensive
502 characterization of beer polyphenols by high resolution mass spectrometry
503 (LC-ESI-LTQ-Orbitrap-MS). Food Chem 169:336–343.
504 https://doi.org/0.1016/j.foodchem.2014.07.154

505 Qiu S, Yang W, Shi X, et al (2015) A green protocol for efficient discovery of novel natural
506 compounds: characterization of new ginsenosides from the stems and leaves of Panax
507 ginseng as a case study. Anal Chim Acta 893:65–76.
508 https://doi.org/10.1016/j.aca.2015.08.048

509 Song C, Jiao C, Jin Q, et al (2020) Metabolomics analysis of nitrogen-containing metabolites
510 between two Dendrobium plants. Physiol Mol Biol Plants.
511 https://doi.org/10.1007/s12298-020-00822-1

512 Suzuki Y, Choi KJ, Uchida K, et al (2004) Arginyl-fructosyl-glucose and Arginyl-fructose,
513 Compounds Related to Browning Reaction in the Model System of Steaming and
514 Heat-drying Processes for the Preparation of Red Ginseng. J Ginseng Res 28:143-148.
515 doi:10.5142/JGR.2004.28.3.143

516 Xu J, Han Q, Li S, et al (2013) Chemistry, bioactivity and quality control of Dendrobium, a
517 commonly used tonic herb in traditional Chinese medicine. Phytochem Rev 12:341–367.
518 https://doi.org/10.1007/s11101-013-9310-8

519 Xu J, Zhao W, Qian Z, et al (2010) Fast determination of five components of coumarin, alkaloids
520 and bibenzyls in Dendrobium spp. using pressurized liquid extraction and
521 ultra-performance liquid chromatography. J Sep Sci 33:1580–1586.
522 https://doi.org/10.1002/jssc.201000034

523 Yan L, Wang X, Liu H, et al (2015) The Genome of Dendrobium officinale Illuminates the
524 Biology of the Important Traditional Chinese Orchid Herb. Mol Plant 8:922–934.
525 https://doi.org/10.1016/j.molp.2014.12.011

526 Zhang J, He C, Wu K, et al (2016) Transcriptome analysis of dendrobium officinale and its
527 application to the identification of genes associated with polysaccharide synthesis. Front
528 Plant Sci 7:. https://doi.org/10.3389/fpls.2016.00005

529 Zhang X, Huang H, Liang X, et al (2009) Analysis of Amaryllidaceae alkaloids from Crinum by
530 high-performance liquid chromatography coupled with electrospray ionization tandem mass
531 spectrometry. Rapid Commun Mass Spectrom 23:2903–2916.
532 https://doi.org/10.1002/rcm.4205

533 # Figure captions

534 **Fig. 1**. The fresh weight and alkaloid contents of *D. officinale* treated with 100 μM MeJA.

535 **Fig. 2**. The mass spectra of tropine and 2,3-dihydroxynortropane. (a) The MS^2 spectrum of tropine,
536 (b) the MS^2 spectrum of 2,3-dihydroxynortropane or an isomer, and (c) the MS^3 spectrum of
537 2,3-dihydroxynortropane or an isomer.

538 **Fig. 3**. The mass spectra of alamaridine and 1,2-dihydro-*O*-methyltazettine. (a) The MS^2 spectrum
539 of alamaridine, (b) the MS^3 spectrum of alamaridine, (c) the MS^2 spectrum of
540 1,2-dihydro-*O*-methyltazettine, and (d) the MS^3 spectrum of 1,2-dihydro-*O*-methyltazettine.

541 **Fig. 4.** The mass spectra of methyllagerine *N*-oxide and meefarnine B. (a) The MS^2 spectrum of
542 methyllagerine *N*-oxide, (b) the MS^2 spectrum of meefarnine B, and (c) the MS^3 spectrum of
543 meefarnine B.

544 **Fig. 5**. The putative fragmentation pathway of anapheline.

545 **Fig. 6**. The mass spectra of the guanidines. (a) The MS^2 spectrum of 4-guanidinobutanoic acid, (b)
546 the MS^3 spectrum of 4-guanidinobutanoic acid, (c) the MS^2 spectrum of cyclocimipronidine, (d)
547 the MS^3 spectrum of cyclocimipronidine, (e) the MS^2 spectrum of *N-tert*-butyloxycarbonyl
548 guanidine, and (f) the MS^3 spectrum of *N-tert*-butyloxycarbonyl guanidine.

549 **Fig. 7**. The putative metabolic network of alkaloids and precursors. The red words denote the
550 identified compounds. The blue words denote the metabolites. The purple words denote the
551 enzymes. The solid arrows denote one-step reactions, and the dashed arrows denote multiple
552 reactions.

553 F**ig. S1**. The mass spectrum of *D. officinale* extract with the standards. (a) The total ion current
554 chromatogram of the methanol extract from *D. officinale* spiked with standards, (b) the extracted
555 ion current chromatogram of *m/z* 311.1738, and (c) the extracted ion current chromatogram of *m/z*
556 609.2772.

557 **Fig. S2**. The putative fragmentation pathway of sarpagine. π denotes π-bond dissociation; i
558 denotes inductive cleavage; rH_R denotes charge-remote rearrangement; rH_B denotes
559 α,β-charge-site rearrangement; rH_C denotes γ-charge-site rearrangement; and $rH_{1,2}$ denotes
560 radical-site rearrangement.

561 **Fig. S3**. The putative fragmentation pathway of reserpine. π denotes π-bond dissociation; i denotes
562 inductive cleavage; rH_R denotes charge-remote rearrangement; and rH_C denotes γ-charge-site
563 rearrangement.

564 **Fig. S4**. The chromatogram and mass spectra of anapheline. (a) The extracted ion chromatogram
565 of anapheline, (b) the MS spectrum of anapheline, (c) the MS^2 spectrum of anapheline, and (d) the
566 MS^3 spectrum of anapheline.

567 **Fig. S5**. The mass spectra of nucleotides and derivatives. (a) The MS^2 spectrum of
568 2-hydroxyadenine, (b) the MS^3 spectrum of 2-hydroxyadenine, (c) the MS^2 spectrum of adenosine,
569 (d) the MS^3 spectrum of adenosine, (e) the MS^2 spectrum of guanosine, (f) the MS^3 spectrum of
570 guanosine, (g) the MS^2 spectrum of 1-methyladenosine, (h) the MS^3 spectrum of
571 1-methyladenosine, (i) the MS^2 spectrum of cytidine, and (j) the MS^3 spectrum of cytidine.

572 **Fig. S6**. The mass spectra of sphingolipids. (a) The MS^2 spectrum of 2-amino-1,3- hexadecanediol,
573 (b) the MS^3 spectrum of 2-amino-1,3- hexadecanediol, (c) the MS^2 spectrum of

2-amino-3-tetradecanol, (d) the MS^3 spectrum of 2-amino-3-tetradecanol, (e) the MS^2 spectrum of 2-amino-1,3,4-octadecanetriol, (f) the MS^3 spectrum of 2-amino-1,3,4-octadecanetriol, (g) the MS^2 spectrum of 2-amino-1,3,4- hexadecanetriol, and (h) the MS^3 spectrum of 2-amino-1,3,4-hexadecanetriol.

Fig. S7. The mass spectra of amino acids and their derivatives. (a) The MS^2 spectrum of 4-hydroxy-L-threonine, (b) the MS^2 spectrum of urocanic acid, (c) the MS^2 spectrum of N^2-fructopyranosylarginine, (d) the MS^3 spectrum of N^2-fructopyranosylarginine, (e) the MS^2 spectrum of *N*-methylarginine, (f) the MS^3 spectrum of *N*-methylarginine, (g) the MS^2 spectrum of N^{α}-acetylarginine, (h) the MS^3 spectrum of N^{α}-acetylarginine, (i) the MS^2 spectrum of N^2-(3-hydroxysuccinoyl)arginine, and (j) the MS^3 spectrum of N^2-(3-hydroxysuccinoyl)arginine.

Fig. S8. The comparative mass spectrum of some isomers. (a) The MS^2 spectrum of L-homophenylalanine, (b) the MS^3 spectrum of L-homophenylalanine, (c) the MS^2 spectrum of β-phenyl-γ-aminobutyric acid, (d) the MS^3 spectrum of β-phenyl-γ-aminobutyric acid, (e) the MS^2 spectrum of carbetamide, (f) the MS^3 spectrum of carbetamide, (g) the MS^2 spectrum of N^{δ}-benzoylornithine, and (h) the MS^3 spectrum of N^{δ}-benzoylornithine.

Fig. S9. The mass spectra of nitrogen-containing glycosides. (a) The MS^2 spectrum of 5'-*O*-*β*-D-glucosylpyridoxine, (b) the MS^2 spectrum of 4-*O*-*β*-D-glucopyranoside-2,4-benzoxazolediol, (c) the MS^3 spectrum of 4-*O*-*β*-D-glucopyranoside-2,4-benzoxazolediol, (d) the MS^2 spectrum of *O*-(tri-*O*-acetyl-α-L-rhamnopyranoside)-(4-hydroxy benzyl)methylcarbamic acid, (e) the MS^3 spectrum of *O*-(tri-*O*-acetyl-*α*-L-rhamnopyranoside)-(4-hydroxy benzyl)methylcarbamic acid, (f) the MS^2 spectrum of passicapsin, and (g) the MS^3 spectrum of passicapsin.

Table S1. Identification of the main chemical compounds from *D.officinale*

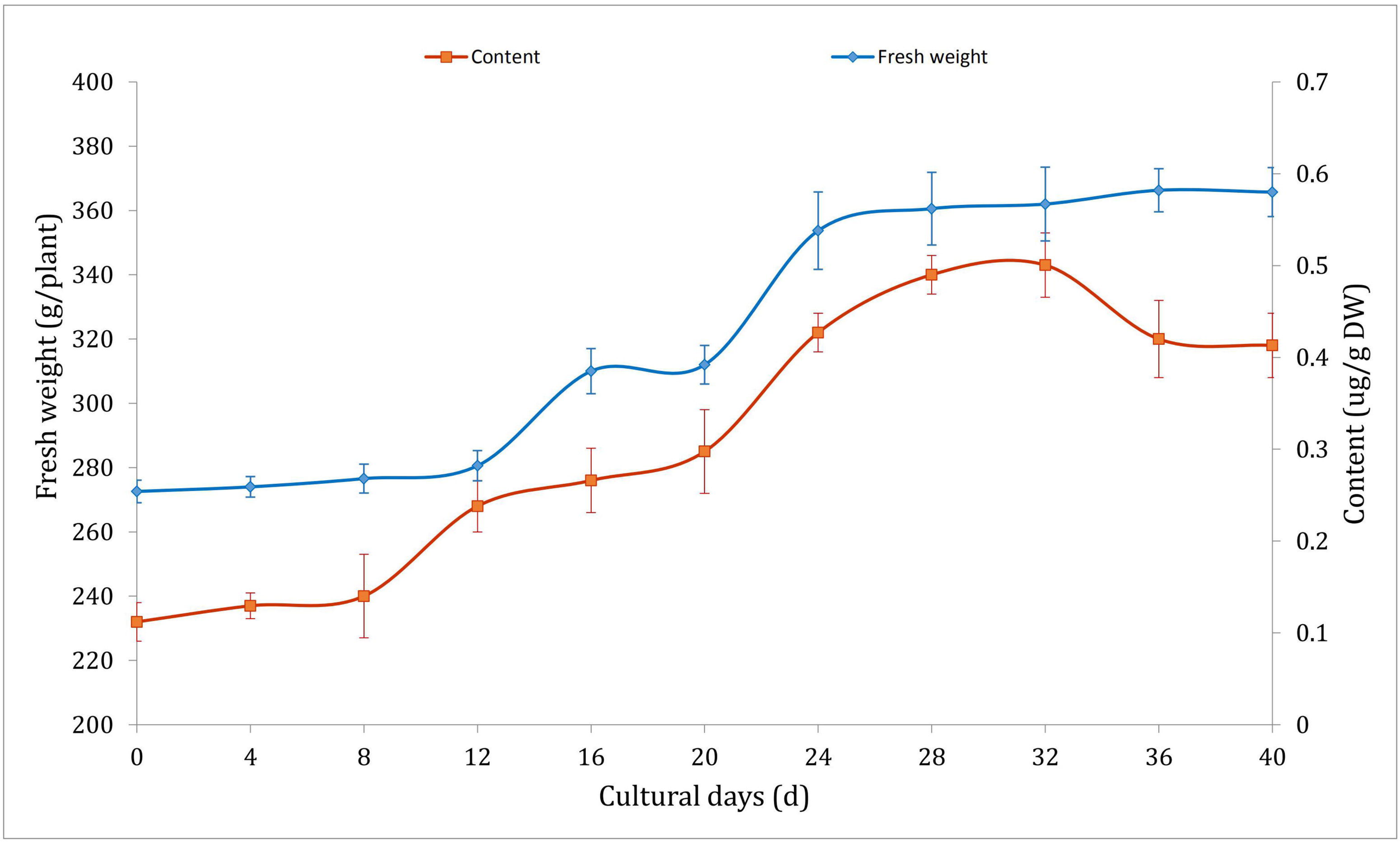
Content
Fresh weight
Fresh weight (g/plant)
Content (ug/g DW)
Cultural days (d)
400
380
360
340
320
300
280
260
240
220
200
0.7
0.6
0.5
0.4
0.3
0.2
0.1
0
0
4
8
12
16
20
24
28
32
36
40

a

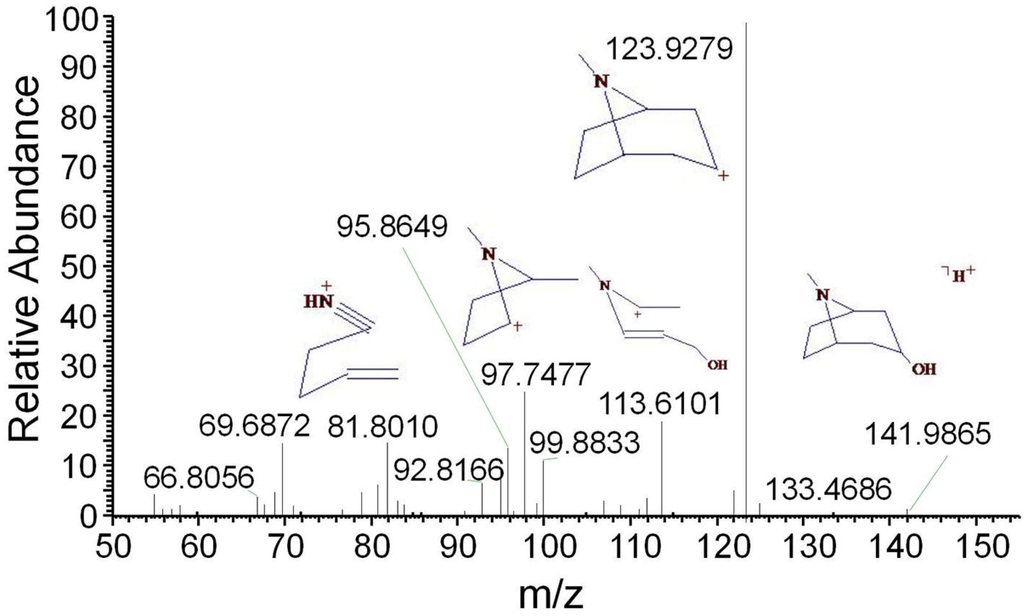
Relative Abundance
m/z
123.9279
95.8649
97.7477
113.6101
69.6872
81.8010
99.8833
141.9865
66.8056
92.8166
133.4686

b

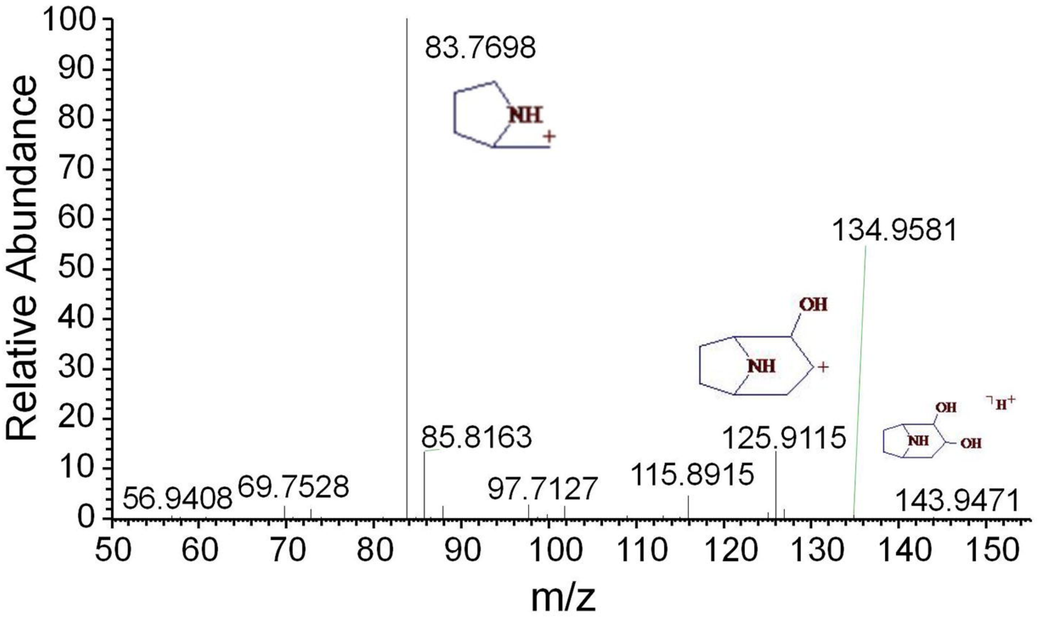
Relative Abundance
m/z
83.7698
134.9581
85.8163
125.9115
115.8915
56.9408
69.7528
97.7127
143.9471

c

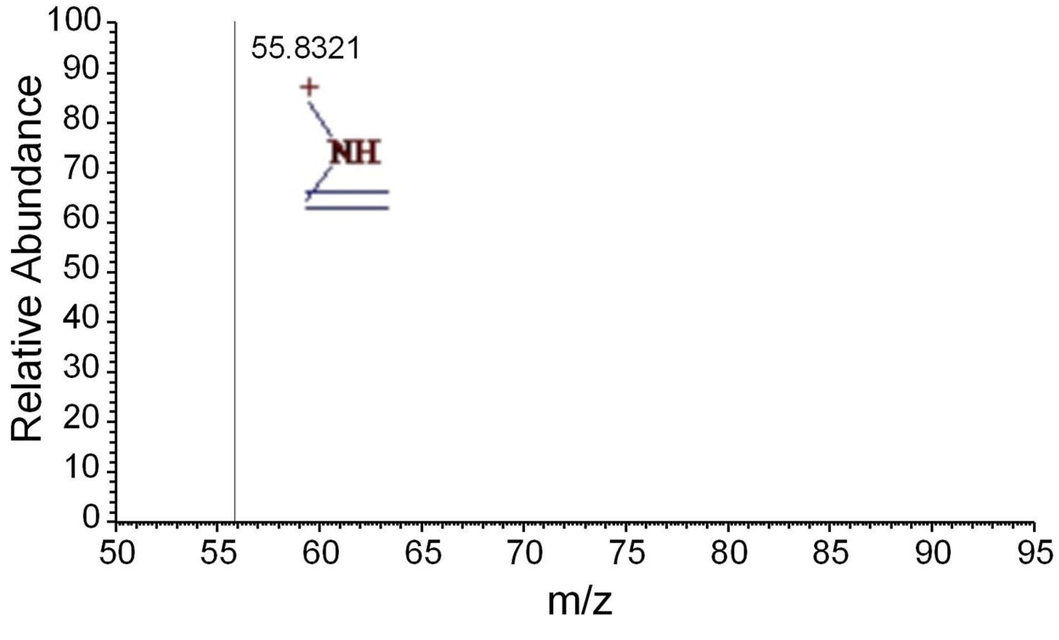
Relative Abundance
m/z
55.8321

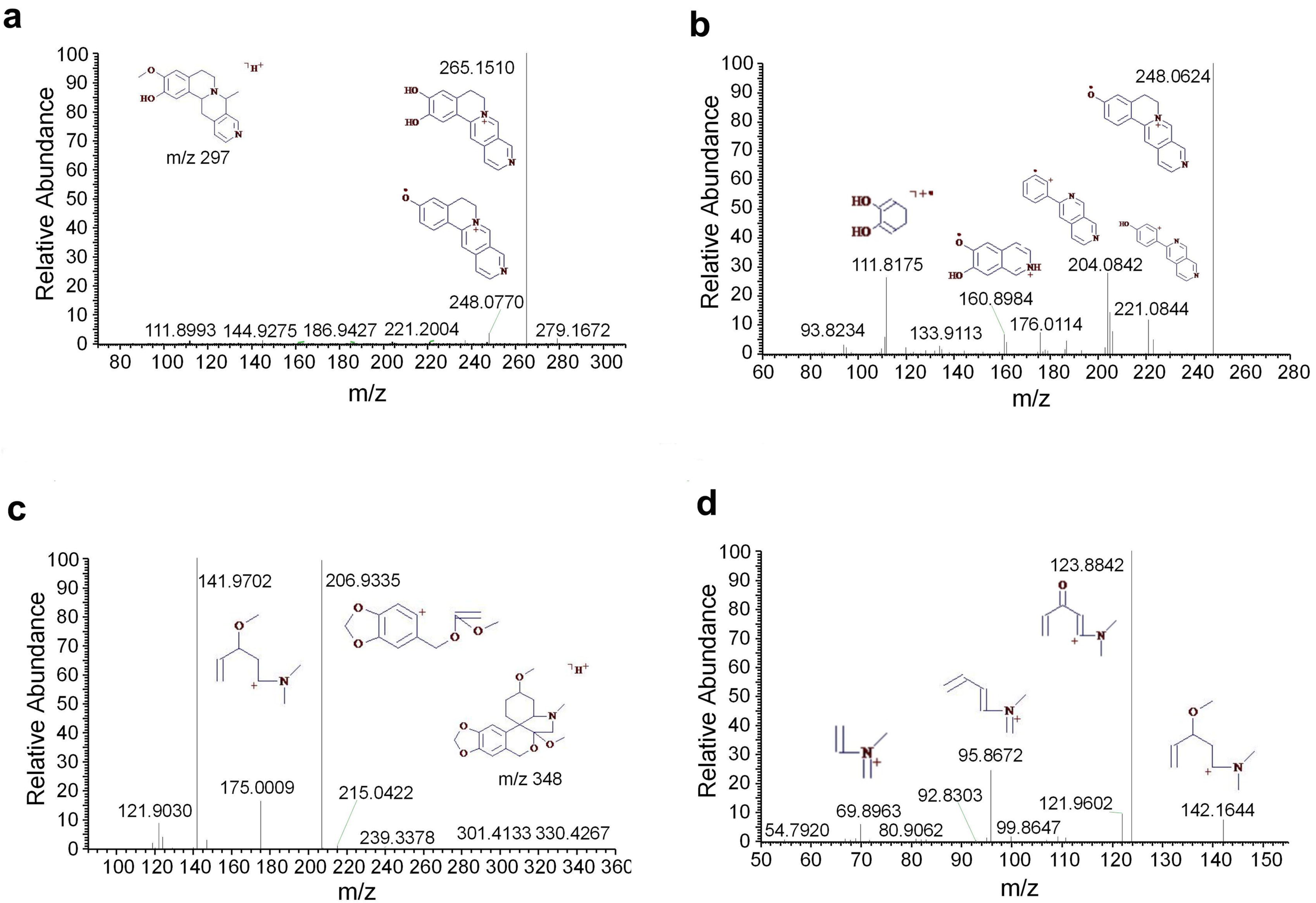
a
Relative Abundance
m/z
m/z 297
265.1510
248.0770
111.8993
144.9275
186.9427
221.2004
279.1672
b
Relative Abundance
m/z
248.0624
111.8175
204.0842
160.8984
221.0844
93.8234
133.9113
176.0114
c
Relative Abundance
m/z
141.9702
206.9335
m/z 348
121.9030
175.0009
215.0422
239.3378
301.4133
330.4267
d
Relative Abundance
m/z
123.8842
95.8672
92.8303
121.9602
142.1644
69.8963
54.7920
80.9062
99.8647

a

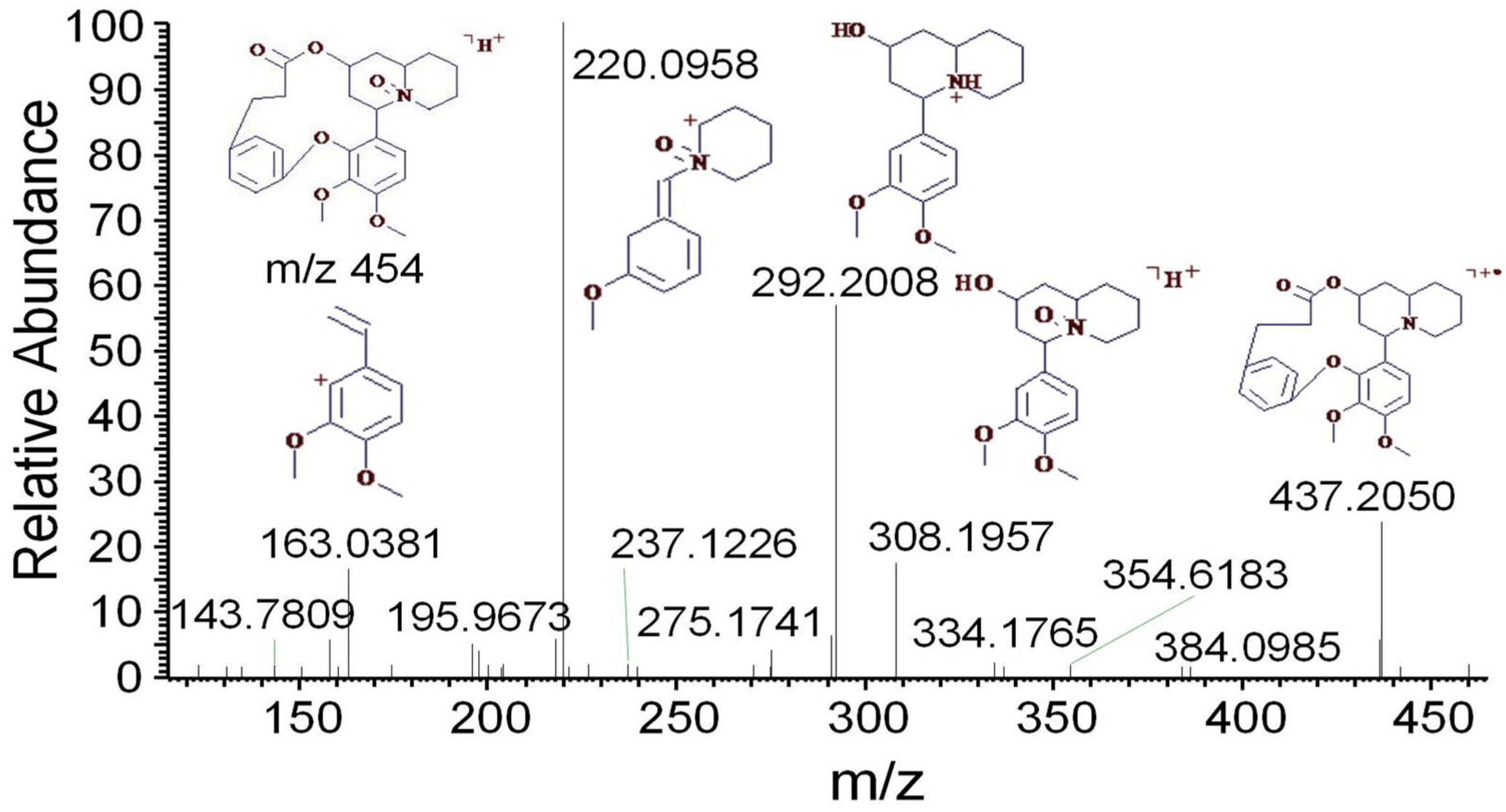
Relative Abundance
m/z
m/z 454
220.0958
292.2008
437.2050
163.0381
237.1226
308.1957
354.6183
143.7809
195.9673
275.1741
334.1765
384.0985

b

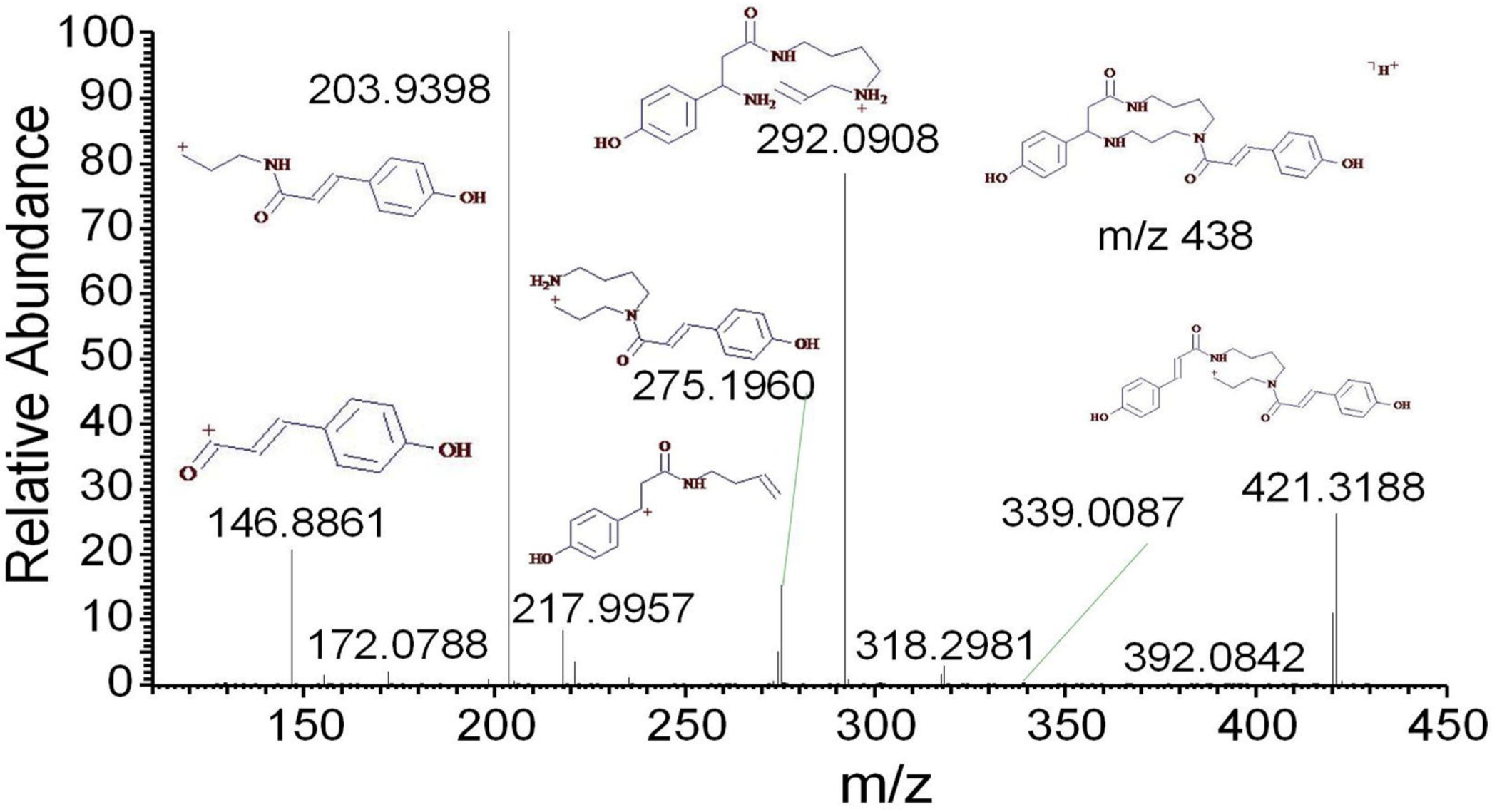
Relative Abundance
m/z
203.9398
292.0908
m/z 438
275.1960
146.8861
217.9957
339.0087
421.3188
172.0788
318.2981
392.0842

c

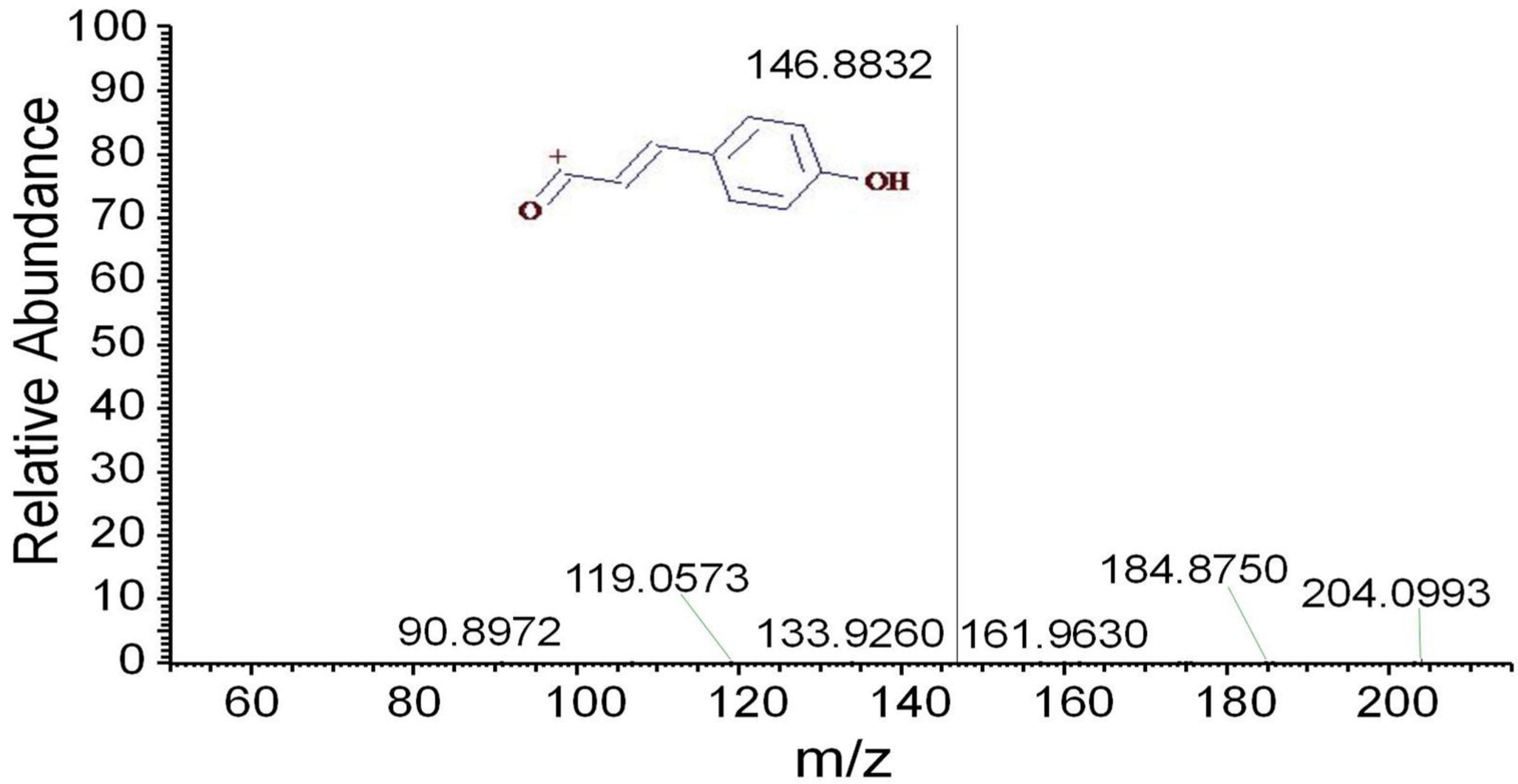
Relative Abundance
m/z
146.8832
119.0573
184.8750
204.0993
90.8972
133.9260
161.9630

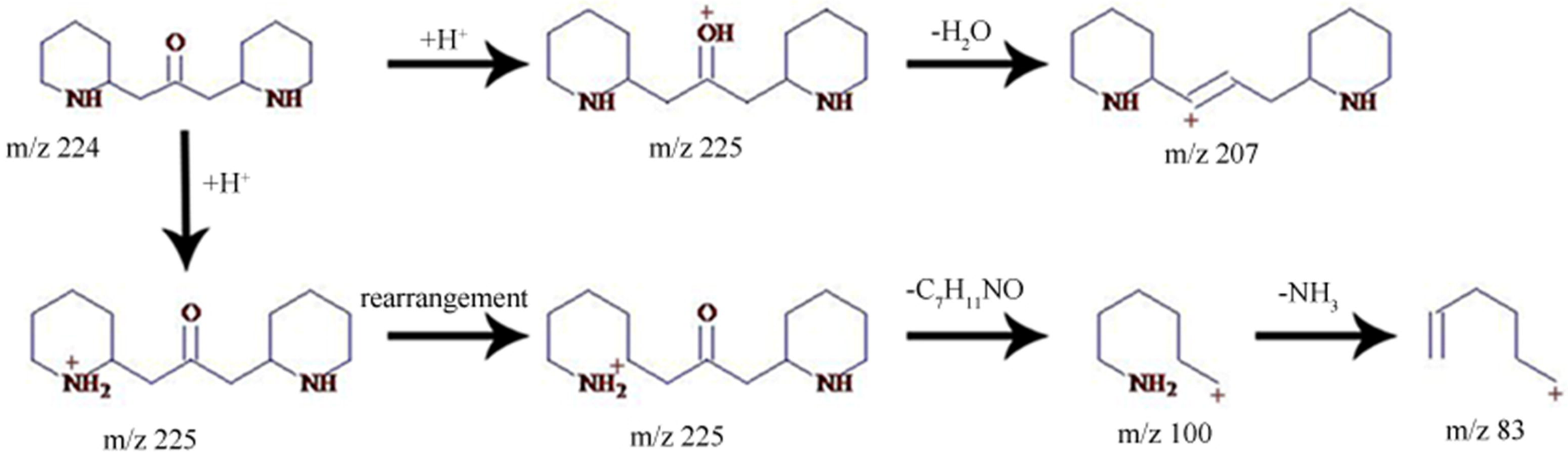
m/z 224
+H+
m/z 225
-H2O
m/z 207
+H+
m/z 225
rearrangement
m/z 225
-C7H11NO
m/z 100
-NH3
m/z 83

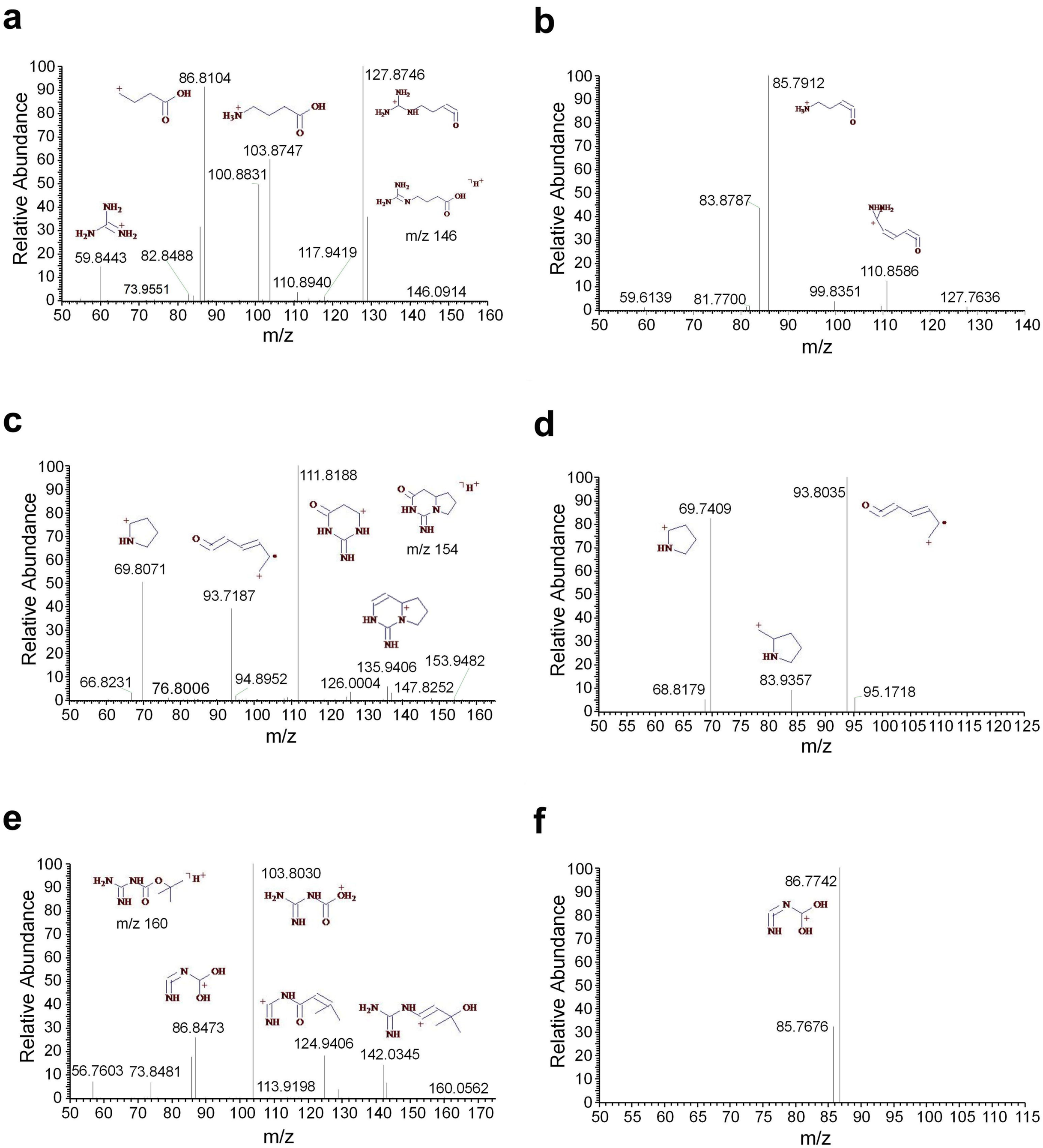
a
Relative Abundance
m/z
86.8104
127.8746
103.8747
100.8831
59.8443
82.8488
73.9551
110.8940
117.9419
146.0914
m/z 146
b
Relative Abundance
m/z
85.7912
83.8787
110.8586
59.6139
81.7700
99.8351
127.7636
c
Relative Abundance
m/z
111.8188
69.8071
93.7187
m/z 154
66.8231
76.8006
94.8952
126.0004
135.9406
147.8252
153.9482
d
Relative Abundance
m/z
93.8035
69.7409
83.9357
68.8179
95.1718
e
Relative Abundance
m/z
103.8030
m/z 160
86.8473
56.7603
73.8481
124.9406
142.0345
113.9198
160.0562
f
Relative Abundance
m/z
86.7742
85.7676

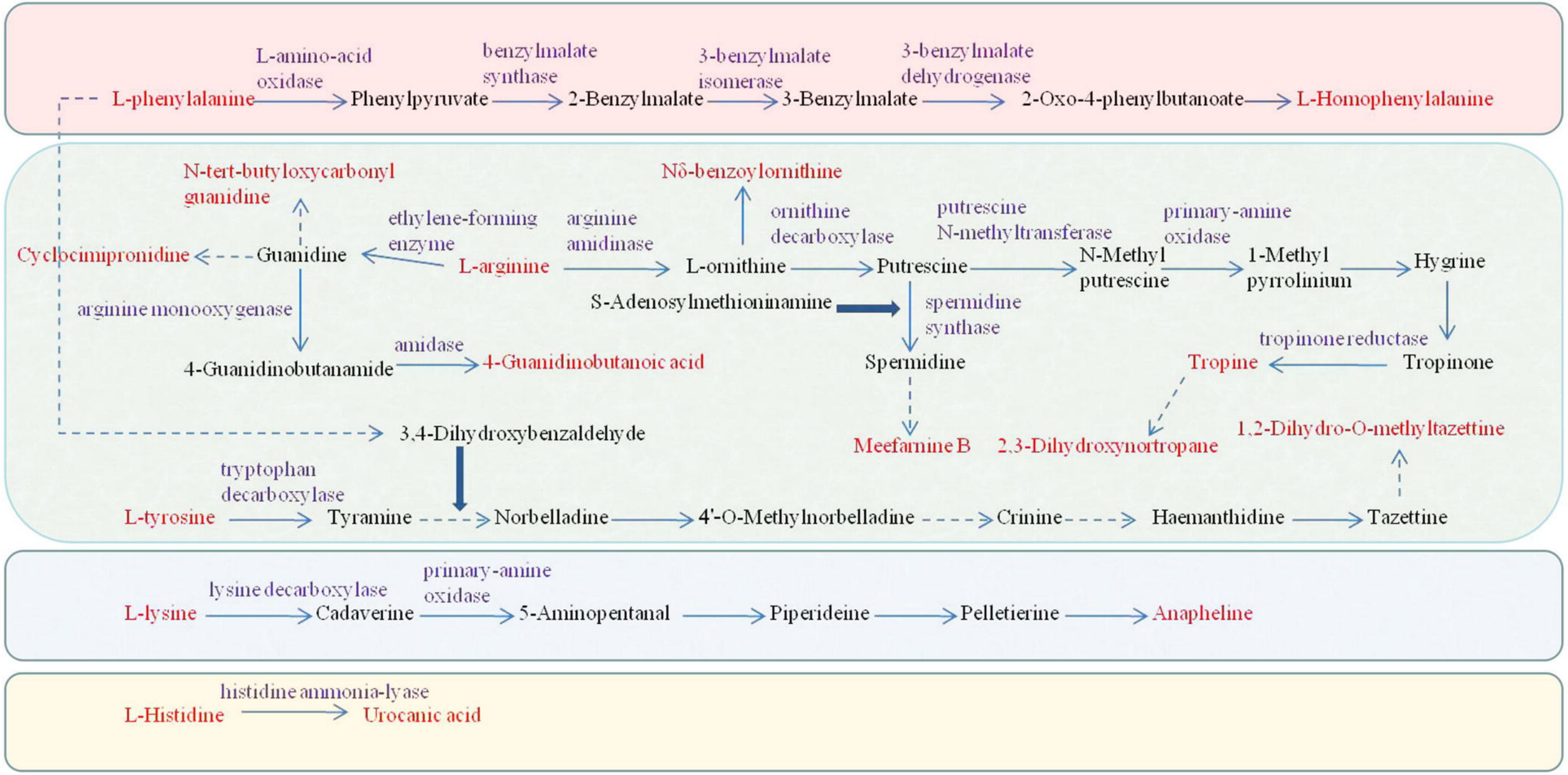
L-phenylalanine
L-amino-acid oxidase
Phenylpyruvate
benzylmalate synthase
2-Benzylmalate
3-benzylmalate isomerase
3-Benzylmalate
3-benzylmalate dehydrogenase
2-Oxo-4-phenylbutanoate
L-Homophenylalanine
N-tert-butyloxycarbonyl guanidine
Nδ-benzoylornithine
ethylene-forming enzyme
arginine amidinase
ornithine decarboxylase
putrescine N-methyltransferase
primary-amine oxidase
Cyclocimipronidine
Guanidine
L-arginine
L-ornithine
Putrescine
N-Methyl putrescine
1-Methyl pyrrolinium
Hygrine
arginine monooxygenase
S-Adenosylmethioninamine
spermidine synthase
amidase
tropinone reductase
4-Guanidinobutanamide
4-Guanidinobutanoic acid
Spermidine
Tropine
Tropinone
3,4-Dihydroxybenzaldehyde
Meefarnine B
2,3-Dihydroxynortropane
1,2-Dihydro-O-methyltazettine
tryptophan decarboxylase
L-tyrosine
Tyramine
Norbelladine
4'-O-Methylnorbelladine
Crinine
Haemanthidine
Tazettine
lysine decarboxylase
primary-amine oxidase
L-lysine
Cadaverine
5-Aminopentanal
Piperideine
Pelletierine
Anapheline
histidine ammonia-lyase
L-Histidine
Urocanic acid